Agricultural Water Management 269 (2022) 107713

Contents lists available at ScienceDirect

Agricultural Water Management

journal homepage: www.elsevier.com/locate/agwat

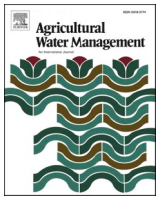

Developing stage-specific drought vulnerability curves for maize: The case study of the Po River basin

Beatrice Monteleone [a,*], Iolanda Borzí [b], Brunella Bonaccorso [b], Mario Martina [a]

[a] University School for Advanced Studies Pavia, Piazza della Vittoria 15, 27100 Pavia, Italy
[b] Department of Engineering, University of Messina, Contrada di Dio, Villaggio Sant'Agata, 98166 Messina, Italy

ARTICLE INFO

Handling Editor: Dr R Thompson

Keywords:
Vulnerability curves
Maize
Water stress
Po River basin

ABSTRACT

Drought and water stress negatively affect many human activities, with agriculture playing a crucial role in ensuring food security. The drought vulnerability assessment of agricultural systems has been widely investigated in the past and the relationship between drought hazard and losses has been traditionally expressed through vulnerability curves. This study develops maize drought vulnerability curves tailored to the context of the Po River Basin (Northern Italy) which is the largest Italian agricultural area and accounts for 35% of national crop production. The curves express the relationship between crop water stress and maize yield losses. Four crop growth stages are considered (establishment, vegetative, flowering and yield formation) since the sensitivity of maize to water stress is strictly related with the plant growth stage. In addition, the influence of soil texture on the maize response to water stress is investigated. The Agricultural Production System sIMulator (APSIM) is used to simulate the crop yield and the water stress. APSIM is calibrated on observed yield and the model skill in reproducing maize yield is satisfactorily verified (Pearson correlation coefficient equals to 0.87). Flowering is the most sensitive stage to water deficit independently from the soil texture, while the yield formation phase is most sensitive to water stress than the vegetative in the case of Loam soils. The achieved results suggest the importance of the use of appropriate irrigation strategies. Water should be provided to maize in case of a water stress during the flowering phase to avoid irreparable yield losses.

1. Introduction

Impacts from recent climate-related hazards have revealed the substantial vulnerability of many human systems to floods and droughts (Cesarini et al., 2021; Lu et al., 2021; von Christierson et al., 2012). Drought affects a wide range of human systems and economic activities, such as power generation, tourism and obviously agriculture. The agricultural sector is particularly exposed to precipitation shortages, high temperatures and insufficient soil moisture, which lead to yield losses and crop failure (Monteleone et al., 2020). The Food and Agriculture Organization estimated that worldwide 83% of all documented drought-caused economic losses were absorbed by agriculture, with a price tag of $29 billion in developing countries (andAgricultureOrganization, 2012,andAgricultureOrganization, 2017,andAgricultureOrganization, 2017). The assessment of drought vulnerability of the agricultural sector has been widely investigated in the past. Already twenty years ago Wilhelmi and Wilhite (2002) proposed a framework to derive an agricultural drought vulnerability map through developing a numerical weighting scheme to evaluate the drought potential of various biophysical and social factors. Understanding the response of crops to droughts and water deficit is of key importance to estimate the effects of future droughts on agricultural production. Various studies explored the response of crops to drought: Yang et al. (2020) evaluated the response of winter wheat to water deficit in the North China Plain, Kamara et al. (2003) investigated the response of different maize hybrids to water stress in Sudan, Korres et al. (2017) reviewed drought impacts on rice production and proposed mitigation strategies to deal with the increase in drought frequency that is expected in a climate change context. Traditionally, the relationship between drought hazard and losses is expressed through vulnerability functions (Papathoma-Köhle, 2016), sometimes called drought damage functions. These functions are continuous curves relating the drought intensity, expressed through a drought index or indicator, and the negative effects of the drought (Bachmair et al., 2017). The development of drought vulnerability curves is challenging due to the limited availability of drought damage data (Bachmair et al., 2016). However, the attention on

* Corresponding author.
E-mail address: beatrice.monteleone@iusspavia.it (B. Monteleone).

https://doi.org/10.1016/j.agwat.2022.107713
Received 10 February 2022; Received in revised form 22 April 2022; Accepted 7 May 2022
Available online 16 May 2022

Table 1
List of studies implementing crop drought vulnerability curves. List and details on the studies that shows the implementation of crop drought vulnerability curves.

Reference	Country	Crop	Crop model
Steduto et al. (2012)	Global	Various	None
Guo et al. (2016)	Global	Maize	EPIC
Jayanthi et al. (2014)	Western Sahel	Maize and millet	None
Jia et al. (2012)	China	Maize	EPIC
Kamali et al. (2018)	Sub-Saharan Africa	Maize	EPIC +
Su et al. (2021)	North East USA	Maize	EPIC
Wang et al. (2019)	Northwest of China	Maize	None
Wu et al. (2021)	Europe	Winter wheat	EPIC
Yin et al. (2014)	Global	Maize	G-EPIC
Zhang et al. (2015a, 2015b); Yin et al. (2015)	Global	Wheat, Rice, Maize	G-EPIC
Zhu et al. (2021)	China	Maize	AquaCrop
Naumann et al. (2015)	Europe	Cereals	None
Bennett and Harms (2011)	Australia	Alfalfa, barley, canola, corn, dry bean, grass, potato, sugar beet, soft spring wheat	None

developing these functions for the agricultural sector has increased over the last years. Crop specific drought vulnerability functions have been proposed in various studies. Steduto et al. (2012) proposed linear functions that relate crop yield with the ratio between actual and potential evapotranspiration during various growing stages, which depend on the crop. The methodology was then implemented in the AquaCrop crop model, which is the FAO's crop water productivity simulation model (Food and Agriculture Organization, 2017). The major limitation of the linear functions described by Steduto et al. (2012) and used by the AquaCrop model lies in the fact they are not tailored to a specific geographical context. The crop response to water varies according to the climatic features of the considered area, the soil texture and the crop seasonality. Besides the abovementioned FAO study, further studies implemented crop drought vulnerability functions in specific national or regional contexts (Table 1). In addition, due to the scarcity of yield data, many of the cited studies use crop models to evaluate the relationship between weather and soil variables and crop yield.

Bennett and Harms (2011) applied the methodology described in Allen et al. (1988) to derive linear relationships between crop yield and evapotranspiration for the crops grown in Southern Alberta (Australia); Jia et al. (2012) applied the EPIC (Environmental Policy Integrated Climate) crop model to simulate the physical vulnerability curve of a typical maize variety traditionally planted in China. Jayanthi et al. (2014) applied a probabilistic approach to evaluate agricultural drought risk to maize (Southern Africa) and millet (Western Sahel), using observed yield data retrieved at country level and satellite observations to evaluate drought hazard intensity. Yin et al. (2014) proposed the GEPIC V-R model to construct vulnerability curves through setting irrigation scenarios. The EPIC model is used to evaluate the crop response to environmental parameters. The proposed vulnerability curves show the relationship between a Drought Hazard Index (DHI) and yield loss for many world zones. Zhang et al. (2015a), Yin et al. (2015) and Zhang et al. (2015b) mapped the drought risk of wheat, maize and rice respectively at global level applying the methodology described in Yin et al. (2014), and provided vulnerability functions for different zones around the globe. Naumann et al. (2015) evaluated the relationship between cereal yields and various drought indexes (Standardized Precipitation Index (SPI), Standardized Precipitation Evapotranspiration Index (SPEI) and Reconnaissance Drought Index (RDI) aggregated at 3, 6 and 12 months) in many European countries. The functions proposed in the study have different shapes, which can be explained by each country's specific drought vulnerability or adaptive capacity. Guo et al. (2016) shows a new method based on vulnerability surfaces to assess vulnerability quantitatively and continuously. Global maize drought risk was estimated based on these surfaces. Kamali et al. (2018) developed a physical crop drought vulnerability index through linking the drought exposure index (DEI) with the Crop Sensitivity Index (CSI) in Sub-Saharan Africa. Wang et al. (2019) used a two-dimensional normal information diffusion method to construct the vulnerability relationship between meteorological drought degree (MDD) and relative meteorological yield to obtain the probability distribution curve of MDD and relative meteorological yield in the eastern part of Northwest China. More recently, Su et al. (2021) used precipitation fluctuations and the coefficient of variation (CV) of yield as indicators to construct a vulnerability curve for the CV of yield and precipitation fluctuations in the context of the North-eastern USA. Wu et al. (2021) investigated the vulnerability curve feature extraction and spatial difference analysis method in Europe and took into consideration the European winter wheat. Again, EPIC was the selected crop model. Finally, Zhu et al. (2021) applied the AquaCrop model to simulate the water stress of maize in China under different irrigation scenarios and the corresponding production. This study is highly interesting since it evaluates the effect of water stress occurring at various growth stages on the final crop production. As clearly shown by Steduto et al. (2012), the time of a drought during crop growth plays a significant role in yield reduction. In fact, some stages, such as flowering, are more sensitive to water stress and drought events occurring at that time can result in relevant yield losses. In addition, soil texture plays a relevant influence on crop response to water stress. A proper identification of soil features is then a fundamental issue. Commonly, soil type classification relies on the relative fractions of soil particles of different sizes to establish soil textural class boundaries (Soil Science Division Staff, 2017). The classification is convenient because grain size distribution can be measured relatively easily and can be estimated quickly and accurately in the field. Soil texture classification is traditionally used within agricultural, geotechnical, hydrological, and other related disciplines from the '20s (Davis and Bennett, 1927). The key issue of proper soil textures representation has been approached in different ways in hydrological modelling, characterizing soils with parameters to be calibrated (Borzì et al., 2019; Croke et al., 2002; Jakeman and Hornberger, 1993; Ivković, 2006; Werner et al., 2006) or, in absence of data information, assimilating with catchments with similar characteristics (Blöschl et al., 2013; Viglione et al., 2013), or with the usage of big-scale distributed land surface parameter dataset (Schaperow et al., 2021. Groenendyk et al. (2015) recently focused on the use of soil texture as a proxy for soil hydraulic properties. This has become increasingly common with the growth in coverage and widespread use of global circulation models, which require spatially distributed soil properties over large areas (Saxton et al., 1986; Webb et al., 1993; Wilson and Henderson-Sellers, 1985). Specifically, soil maps have been widely used to identify boundaries where hydraulic properties can be assumed to be constant (Borzì and Bonaccorso, 2021; Borzì et al., 2020; Shaban et al., 2006; Storck et al., 1998) and to provide guidance for parametrization of numerical models. This paper aims at developing crop specific drought vulnerability curves for maize in the context of the Po River basin (Northern Italy). In line with the research of Zhu et al. (2021), the study assesses maize response to water during various crop growth stages to identify the critical periods during which lack of water can have severe impacts in yield losses. The Agricultural Production System sIMulator (APSIM) crop model simulates the yield. APSIM, with respect to AquaCrop, has been specifically designed to provide accurate predictions of crop production in relation to climate, soil and management factor, while addressing the long-term resource management issues. APSIM has been preferred to Aquacrop because the latter is well suited for areas

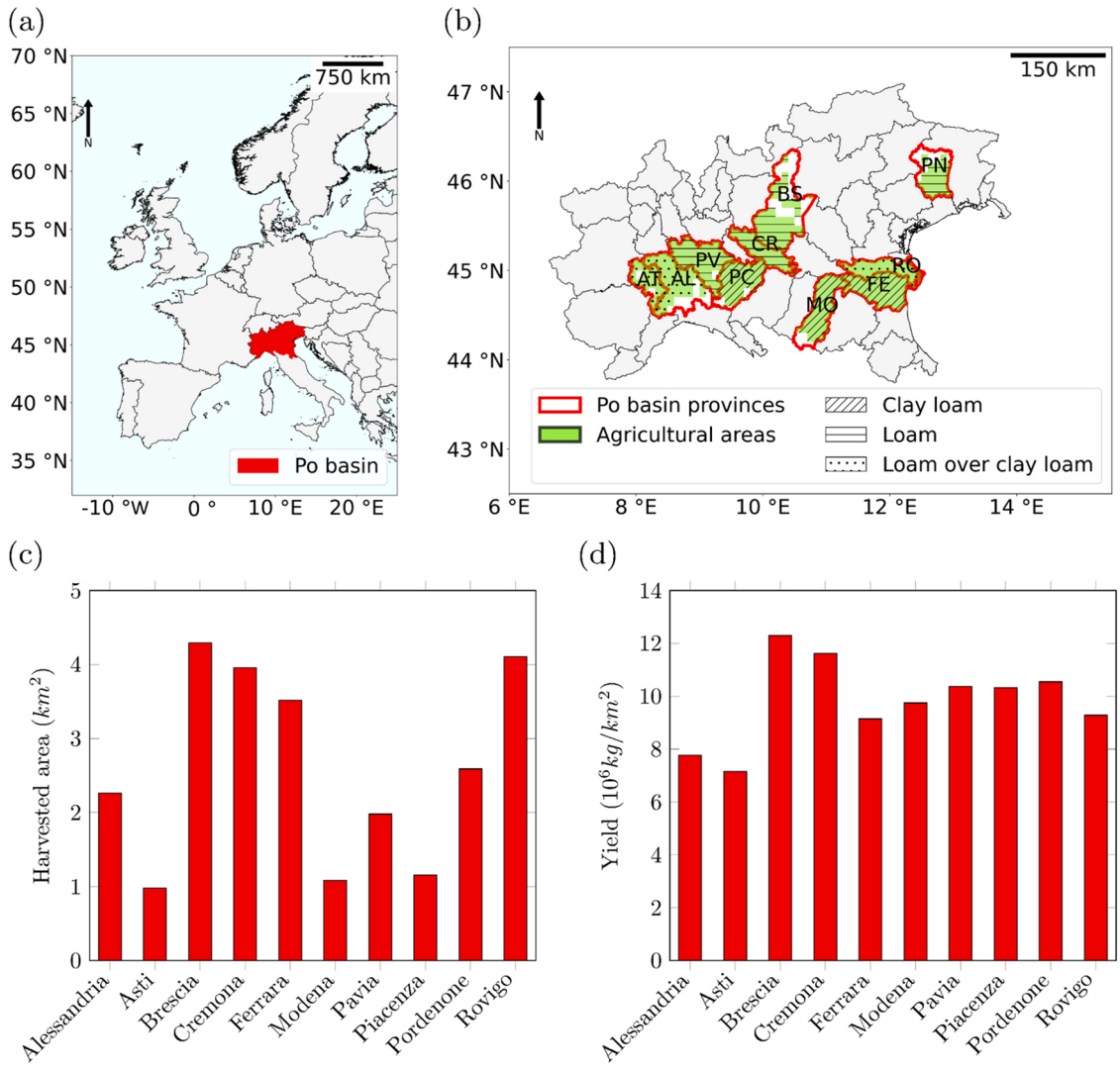

Fig. 1. Location of the case study area (the Po River basin), the provinces of interest, agricultural areas, and harvested area and yield of the provinces. (a) Location of the Po River basin (Italy) inside Europe. (b) Details on the ten provinces considered in the study, their agricultural areas and their soil texture. (c) Average maize harvested area over the 2006–2020 period (d) Average maize yield over the 2006–2020 period.
Data retrieved from Italian National Institute of Statistics (2021) AT: Asti, AL: Alessandria, BS: Brescia, CR: Cremona, FE: Ferrara, MO: Modena, PC: Piacenza, PN: Pordenone, PV: Pavia, RO: Rovigo.

where water is a key limiting factor in crop production, which at present is not the case in the context of the Po River basin. The analyses are conducted at specific stage scale to identify which growth stage is more sensitive to water crises in terms of yield reduction and related water stress. This approach has been chosen in the perspective of practical applications of this study, to support water managers and farmers to a proper and more sustainable resources management during drought. In addition, the influence of soil texture on the crop response to water stress is evaluated. This last aspect has never been considered in the previous studies on crop specific drought vulnerability curves and represents the most innovative feature of the present work. In fact, soil texture plays an important role determining the available crop water and therefore has a critical influence on the final yield (Shaxson and Barber, 2003). Finally, a vulnerability matrix is proposed to classify the crop vulnerability according to the soil texture during the considered crop growth stages. The matrix can be useful to explore the effects of future droughts on maize yield in the various provinces of the Po Valley.

2. Case study

The Po Basin is located in Northern Italy and develops around the Po River, which is the longest river in Italy and flows eastward across northern Italy starting from the Cottian Alps (Fig. 1a). The basin has an extension of about 74,000 km^2, of which about 71,000 km^2 across the Italian territory. The Basin covers seven regions in Italy: Piemonte, Valle d'Aosta, Lombardia, Veneto, Liguria, Emilia-Romagna and the Trento Autonomous Province and has also small areas located in Switzerland and France that have not been considered in the present study. The basin plays a key role in the economy of Italy: it produces 40% of national GDP and consumes 48% of the national produced energy. Around 16 million of people live inside the Basin. The Po valley is the largest agricultural area in Italy and accounts for 35% of Italian agricultural production. The main crops grown in the region are cereals, covering about 85% of the irrigated agricultural area (maize, rice and wheat), and arboreal crops (fruit orchards and horticulture) (Musolino et al., 2018). The basin is characterized by the presence of various climatic zones (Beck et al., 2018). The main one is temperate and characterized by the absence of a dry season and a hot summer. Part of the basin is located on the Alps, and has therefore a cold climate, with no dry season and a warm summer or a Polar climate. The basin has experienced multiple droughts since 1983, as reported by Baronetti et al. (2020), who evaluated the severity and duration of the various drought episodes using both SPI and SPEI.

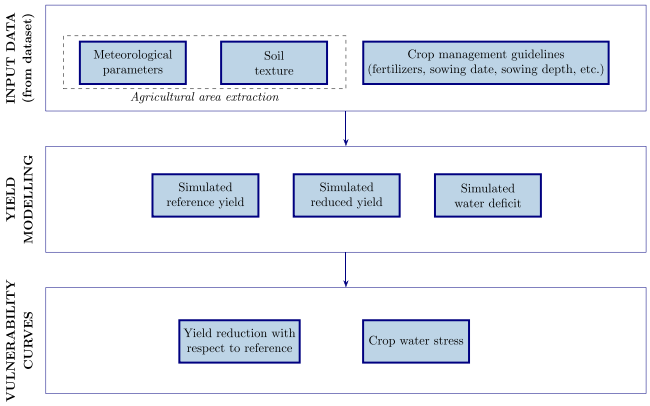

Fig. 2. Flowchart of the proposed methodology. Overview of the input data and the logic sequence of the main steps of the approach followed to develop maize stage- specific maize vulnerability curves. Starting from rainfall data, soil texture and crop management practices retrieved over the agricultural area of the Po basin the reference yield and the reduced yield are simulated. The reference yield is the yield in the absence of any water stress during the entire growing season, the reduced yield is the yield at the end of a season affected by a water deficit in one of the growth stages (establishment, vegetative, flowering and yield formation). The water deficit experienced by the crop is also simulated. Crop water stress is retrieved from the water deficit and the yield reduction with respect to reference yield is derived. These last two parameters are used to derive the curves.

Table 2
Crop management practices. Crop management practices (sowing window, density and depth, row spacing and input of nitrogen (N) fertlizers as reported in the guidelines for farmers drown up by the Lombardy region (Regione Lombardia, 2020a, 2020b).

	Maize
Season	Spring
Sowing window	1–30 April
Sowing density (plants/m^2)	8
Row spacing (mm)	500
Sowing depth (mm)	50
Input of N fertilizer (kg/m^2)	0.024

The long and severe drought from 2003 to 2008 caused relevant impacts to the agricultural sector. The total economic impact of the 2005–2007 drought was estimated to be around 1.850 M€ (Musolino et al., 2017). Climate change projections over the Italian peninsula from the PRUDENCE regional experiments (Palatella et al., 2010) showed that the frequency and the severity of droughts in Northern Italy will increase in the next century due to a decrease in precipitation during critical crop growing seasons (spring and summer). In addition, the analysis done by Crespi et al. (2020) showed a significant drying tendencies in both SPI and SPEI over shorter time windows (20–30 years) starting in 1980 and in 1970 for spring and summer, respectively.

The estimation of drought impacts on agriculture is fundamental to foresee the effects that future droughts will have on the sector, which plays a crucial part in the economy of the area. The main crops produced in the Po Valley are cereals (mainly maize, rice and winter wheat), together with orchards and vineyards. The National census (ISTAT, Italian National Institute of Statistics) reports data on crop production and harvested area over the period from 2006 to 2020 for each province (Italian National Institute of Statistics, 2021). Details on maize harvested area and yield for the ten provinces shown in Fig. 1b, are reported in Fig. 1c and d, respectively.

3. Methodology

In the present study the development of maize drought vulnerability curves specific for the Po River basin context is carried out following the methodological framework shown in Fig. 2. At first the areas suitable for agriculture in the Po Valley are extracted from a land use dataset, then meteorological parameters and soil texture of the agricultural areas are derived for each of the ten considered provinces described in Section 2. Crop management practices traditionally employed in the Po valley are also identified. All the three inputs are used to calibrate the APSIM crop model. The evaluation of the model ability in reproducing observed yield over each province is then assessed. APSIM is calibrated over the period 2006–2011 and validated over the 2012–2020 period. Once that the model skill in reproducing the observed yield is verified, APSIM is used to simulate:

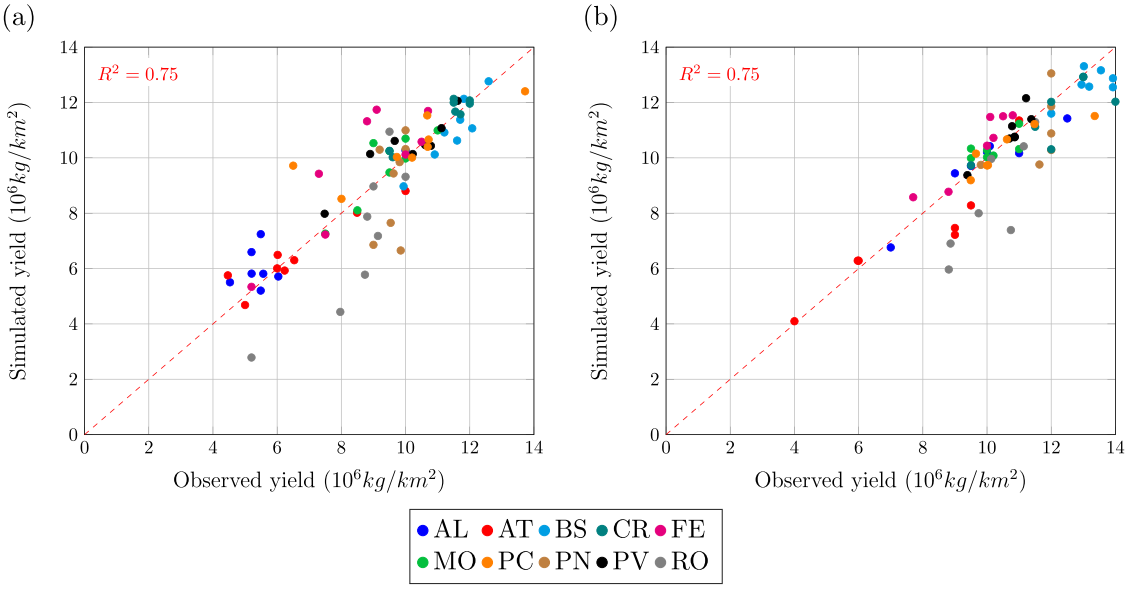

Fig. 3. Performance of the APSIM crop model in reproducing the observed yield in the ten selected provinces. Results of the APSIM calibration (a) and validation (b) over the observed yield retrieved from the Italian national institute of statistics. The correlation coefficient R^2 is reported in red and is equal to 0.75 in both cases with a $p < 0.01$. AT: Asti, AL: Alessandria, BS: Brescia, CR: Cremona, FE: Ferrara, MO: Modena, PC: Piacenza, PN: Pordenone, PV: Pavia, RO: Rovigo.

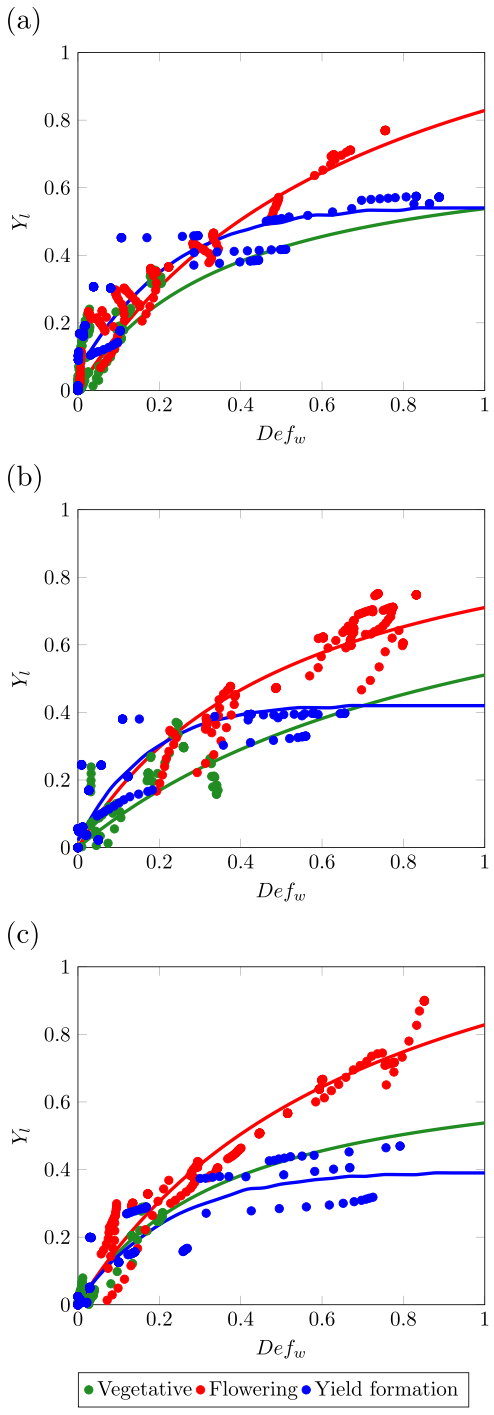

Fig. 4. Stage specific drought vulnerability curves for maize in Rovigo, RO (a), Ferrara, FE (b) and Pavia, PV (c). The green line represents the vegetative stage, the red the flowering and the blue the yield formation phase. The curves have been fitted on the values represented by the dots using the Michaelis-Menten equation for the vegetative and the flowering stage and the asymmetric logistic equation for the yield formation phase. Water deficit, Def_w, going from 0 to 1, is computed as 1 minus the ratio between crop water uptake from soil and crop water demand, while yield loss, Y_l, going from 0 to 1, is computed as 1 minus the ratio between the reduced yield and the reference yield.

(1) a reference yield, i.e., the crop yield in normal conditions at a given location (Jayanthi et al., 2014) in each specific crop growth stage;
(2) a reduced yield, i.e., the crop yield under water stress conditions during a specific crop growth stage;

Table 3
R^2 values relative to the goodness of fit of the data points to the selected functions for the ten considered provinces and the three growth stages.

Province	Vegetative	Flowering	Yield formation
Alessandria	0.943	0.968	0.928
Asti	0.892	0.953	0.903
Brescia	0.890	0.940	0.885
Modena	0.848	0.931	0.881
Rovigo	0.895	0.968	0.912
Pavia	0.951	0.974	0.919
Pordenone	0.849	0.938	0.937
Cremona	0.877	0.970	0.941
Ferrara	0.817	0.908	0.858
Piacenza	0.826	0.950	0.917

(3) the crop water stress during a specific growth stage.

Four crop growth stages are considered as proposed in Food and Agriculture Organization, 2012:

(1) establishment is the period immediately after sowing,
(2) the vegetative phase is the stage in which the crop develops,
(3) flowering includes the flag leaf stage and
(4) yield formation is the final stage in which the maize grain fill.

The following sections provide details about the various steps described in the flowchart.

3.1. Extraction of agricultural areas

Agricultural areas in the Po River basin are identified using the 2018 Corine Land Cover produced in the framework of the Copernicus Land Monitoring Services European Environment Agency (EEA), 2018. Corine Land Cover consists of an inventory of land cover in 44 classes. The map has a 100x100 *m* spatial resolution. Agricultural areas belonging to the classes 'Non irrigated arable land', 'Permanently irrigated land', 'Annual crops associated with permanent crops' and 'Complex cultivation patterns' are extracted from the dataset (Fig. 1b). Only the selected areas are considered suitable for maize and wheat cultivation.

3.2. Meteorological parameters

Daily weather parameters are retrieved from the Ensembles daily gridded Observational dataset (E-OBS) (Cornes et al., 2018). E-OBS has a $10 - km$ grid resolution and provides daily values for multiple weather variables from 1951 to 2020. The dataset is based on the interpolation of measurements directly retrieved from meteorological stations. The stations coverage over the case study area, the Po river basin, is accurate for both rainfall and temperature (Cornes et al., 2018). Weather parameters (rainfall, maximum and minimum daily temperature and radiation) are extracted for the 2006–2020 period and aggregated at province level over the agricultural areas retrieved from the Corine Land Cover.

3.3. Soil texture

Soil texture of the agricultural areas is derived from the International Soil Reference and Information Centre (ISRIC) soil dataset described in Hengl et al. (2017). Soil textures are classified according to the United Stated Department of Agriculture (USDA) methodology (Soil Science Division Staff, 2017), based on the percentage of clay, silt and sand. Seven soil layers are considered in the ISRIC dataset: .

(1) Layer 1: 0–5 cm;
(2) Layer 2: 6–15 cm;
(3) Layer 3: 16–30 cm;
(4) Layer 4: 31–60 cm;

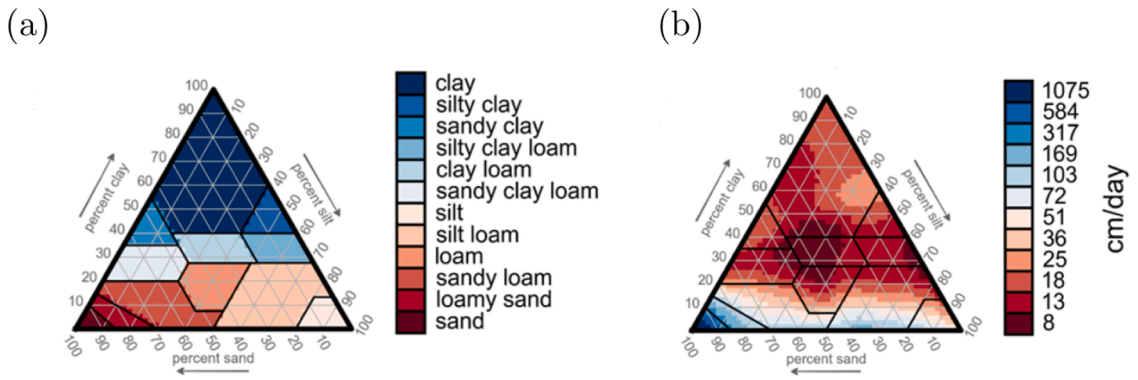

Fig. 5. Soil classification and soil hydraulic conductivity from Groenendyk et al. (2015). Soil classifications plotted based on USDA soil classification (a) and hydraulic conductivity (K_s) on the uppermost 30 cm (b).

(5) Layer 5: 61–100 cm;
(6) Layer 6: 101–200 cm;
(7) Layer 7: deeper than 201 cm.

The soil texture of each soil layer is analysed over the agricultural areas of the ten considered provinces. Fig. 1b shows the soil texture of the agricultural areas of the ten considered provinces. Four provinces have a loam soil over the entire profile, three a clay loam soil over the entire profile and three have a loam over a clay loam soil.

3.4. Crop management practices

Crop management practices in place in the Po Valley are retrieved from a guideline for farmers released by the Lombardy region (Regione Lombardia, 2020a, 2020b). According to that reference, maize is sown in April and harvested between August and September. The recommended sowing density, row spacing, sowing depth and amount of nitrogen fertilizers are summarized in Table 2 and used as set up parameters for model simulations.

3.5. Yield modelling

APSIM is used to simulate crop yield both in ideal conditions, in which the crop has full water availability, and during periods of water stress. APSIM, described in Keating et al. (2003), has been developed by the Agricultural Production Systems Research Unit, a collaborative group made up from the Commonwealth Scientific and Industrial Research Organisation (CSIRO) and Queensland State Government agencies. The crop model has been implemented specifically to provide accurate predictions of crop production in relation to climate. Various parameters are required to initialize a simulation: .

(1) Daily weather data
(2) Soil texture
(3) Crop type
(4) Crop management practices

Daily weather data are obtained from the E-OBS dataset, that has a 10x10 *km* grid resolution. Weather data have been aggregated at province level; average values over agricultural areas of each province have been used to run the simulations. Soil texture was retrieved from the ISRIC dataset and is homogeneous over agricultural areas at province scale. Three generic soils have been selected in APSIM to represent the specific soil texture. The choice is based on the information about soil parameters such as bulk density, field capacity and soil water content reported in Costantini et al. (2013). A Clay Loam generic (n.500) soil has been selected as representative of the clay loam soil texture, a generic loam over clay (n.375) represents the soil texture loam over clay loam and a generic loam (n. 659) soil represents the loam soil texture. Crop management practices are retrieved from the Lombardy region guidelines and described in Table 2.

The outputs provided by the APSIM are: .

(1) Crop yield Y (kg/km^2)
(2) Crop water supply W_s (mm)
(3) Crop water demand W_d (mm)

Based on the input daily weather data (rainfall, maximum and minimum temperature, solar radiation), APSIM calculates effective precipitation purging evapotranspiration from rainfall. The software applies the Hargraves equation:

$$E_p = 0.0022 \quad R_A \quad \delta_T^{'0.5} \quad (T+1) \tag{1}$$

where: R_A is the mean extra-terrestrial radiation (mm/day), which is a function of the latitude; $\delta_T^{'0.5}$ is the difference between mean daily maximum temperature and mean daily minimum temperature for the day of interest in °C; T is the mean air temperature in °C; Crop yield Y is computed according to a crop-specific methodology, that takes into account the characteristics of the considered plants. This approach was first proposed in Monteith and Greenwood (1986). The yield Y is expressed as a function of various parameters:

$$Y = f(D, PAR, f_s, crop\ parameters) \tag{2}$$

where D is the daylength, PAR is the photosyntetically active radiation, f_s is the stress factor,and the crop specific parameters such as the sowing date, the length of its cycle, etc (APSIM, 2018).

Crop water supply of the layer i, $W_s(i)$ is computed according to the SOILWAT2 module (APSIM, 2018) as:

$$W_s(i) = \begin{cases} KL(i)[SW(i) - LL(i)], & \text{if } i \le I-1 \\ \dfrac{D_r(i)}{D_s(i)} KL(i)[SW(i) - LL(i)], & \text{if } i = I \end{cases} \tag{3}$$

where i is the soil layer, I is the deepest soil layer in which roots are present, which depends on the crop type, $SW(i)$ is the soil water content of layer i, $LL(i)$ is the lower limit of plant extractable soil water in layer i, $KL(i)$ is the root water extraction values in layer i, $D_r(i)$ is the root depth within the soil layer i where roots are present, and $D_s(i)$ is the thickness of layer i. The cumulative crop water supply W_s is computed as:

$$W_s = \sum_{i=1}^{I} W_s(i) \tag{4}$$

KL is empirically determined and defines the fraction of available water able to be extracted per day. Root water extraction values must be defined for each combination of crop species and soil type. SW and LL

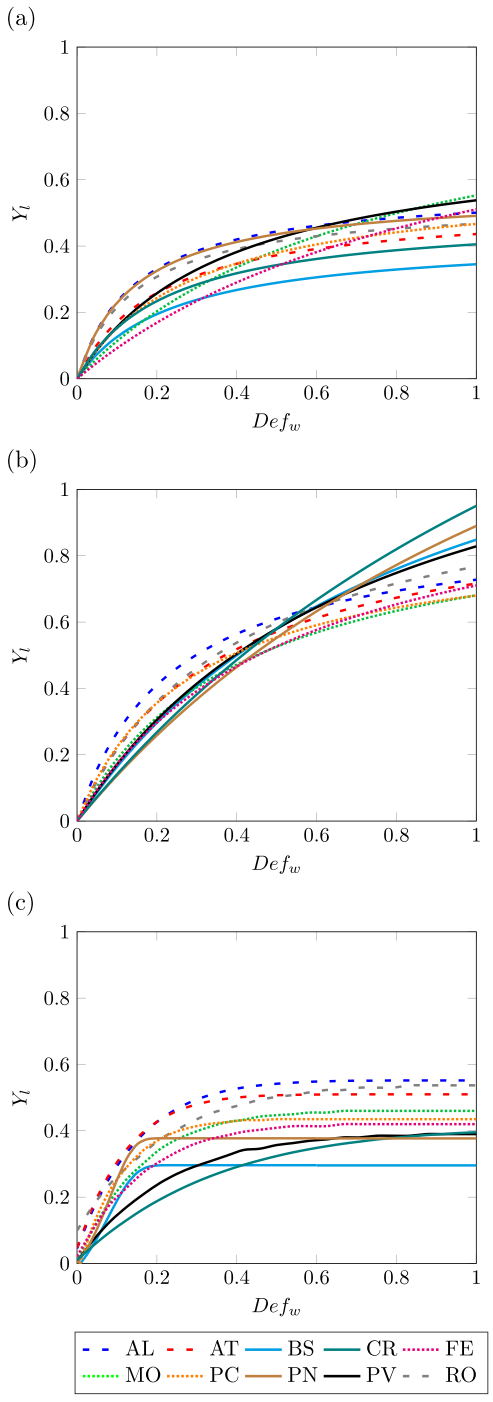

Fig. 6. Maize drought vulnerability curves for the ten considered provinces for the vegetative (a), flowering (b) and yield formation (c) growth stages. Dotted lines indicate provinces with a clay loam soil texture, dashed lines provinces with a loam over clay loam soil texture and continuous lines provinces with a loam soil texture. The curves have been fitted to the data points using the Michaelis-Menten equation for the vegetative and the flowering stage and the asymmetric logistic equation for the yield formation phase. Water deficit, Def_w, going from 0 to 1, is computed as 1 minus the ratio between crop water uptake from soil and crop water demand, while yield loss, Y_l, going from 0 to 1, is computed as 1 minus the ratio between the reduced yield and the reference yield. AT: Asti, AL: Alessandria, BS: Brescia, CR: Cremona, FE: Ferrara, MO: Modena, PC: Piacenza, PN: Pordenone, PV: Pavia, RO: Rovigo.

depend on the soil type, while D_r depend on the crop type.

Crop water demand W_d is computed according to Tanner and Sinclair (2015):

$$W_d = \frac{\Delta Q_r - R}{TE} \tag{5}$$

where R is the respiration rate and is equal to 0 in the used version of APSIM (Zheng et al., 2015), Q_r is the radiation-limited dry-biomass accumulation and TE is the transpiration efficiency. Q_r is derived as follows:

$$\Delta Q_r = Int_{rad} \quad RUE \quad f_d \quad f_s \quad f_c \tag{6}$$

where Int_{rad} is the intercepted radiation, RUE is the radiation use efficiency, f_d is the diffuse factor, f_s is the stress factor and f_c is the carbon dioxide factor. The radiation use efficiency is modelled according to the crop type, while $f_d = 1$ in APSIM 7.10 (Zheng et al., 2015). The stress factor f_s is the minimum value between a temperature factor f_T and a nitrogen factor f_N:

$$f_s = min(f_T, f_N) \tag{7}$$

where the temperature factor is a function of daily mean temperature (Eq. 8) and h_T is a multiplier used to set $f_T = 0$ when $T < 0$ or $T > 35$ and $f_T = 1$ when $10 > T > 25$:

$$f_T = h_T \frac{T_{max} + T_{min}}{2} \tag{8}$$

The nitrogen stress factor is the difference between leaf nitrogen concentration and leaf minimum and critical nitrogen concentration:

$$f_N = R_N \quad \sum \frac{C_N - C_{N,min}}{C_{N,crit} - C_{N,min}} \tag{9}$$

where R_N is a multiplier for nitrogen deficit effect on phenology and is equal to 1.5 (Zheng et al., 2015) and C_N is the leaf nitrogen concentration, $C_{N,min}$ is the minimum leaf nitrogen concentration and $C_{N,crit}$ is the critical leaf nitrogen concentration (Zheng et al., 2015).

The carbon factor f_C is calculated by a function of environmental CO_2 concentration (C, ppm) and daily mean temperature (T_{mean}) as published by Reyenga et al. (1999):

$$f_C = \frac{(C - C_i)(350 + 2C_i)}{(C + 2C_i)(350 - C_i)} \tag{10}$$

in which C_i is a temperature dependant CO_2 compensation point equal to

$$C_i = (163 - T_{mean})/(5 - 0.1 \quad \mathrm{T_{mean}}) \tag{11}$$

The transpiration efficiency TE is derived according to the following equation:

$$TE = f_{C,TE} \frac{f_{TE}}{VPD} \tag{12}$$

where $f_{C,TE}$ is the CO_2 factor for transpiration efficiency, which is a function of carbon dioxide concentration that linearly increases from 1 to 1.37 when CO_2 concentration increases from 350 ppm to 700 ppm (Reyenga et al., 1999), f_{TE} is the coefficient of transpiration efficiency that varies in relation with the growth stage, and VPD is the vapour pressure deficit derived as in Tanner and Sinclair (2015).

Finally, the water uptake W_u of the crop is the minimum between the soil water supply W_s and the crop water demand W_d.

$$W_u = min(W_s, W_d) \tag{13}$$

The crop water deficit f_s is given by:

$$f_s = \frac{W_u}{W_d} \tag{14}$$

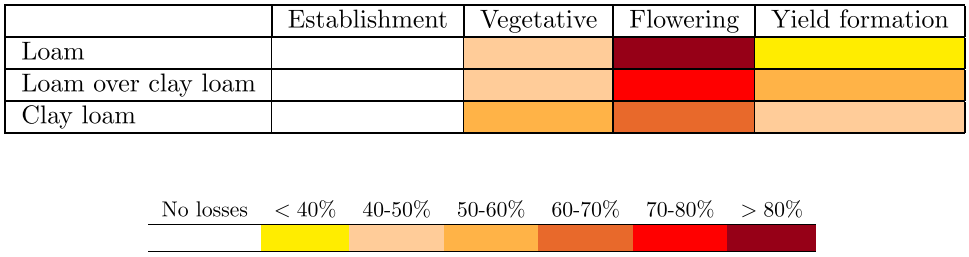

Fig. 7. Vulnerability matrix. The matrix shows the sensitivity to water stress of the individual growth stages (establishment, vegetative, flowering and yield formation) with respect to the soil textures of the ten considered provinces (loam, loam over clay loam and clay loam). Mean Values are used to derive the yield losses expressed in percentage.

Table A.1
Constants of the maize vulnerability curves for the ten considered provinces and the three maize growth stages. Constants of the Michaelis-Menten equation for the vegetative phase (g1, h1) and the flowering phase (g2, h2) and for the asymmetric logistic equation (a,b,c and d) for the ten considered provinces. The vulnerability curves express the relationship between water deficit Def_w (1 minus the ratio between the soil water supply and the crop water demand) and the yield loss Y_l (1 minus the ratio between the reduced yield and the reference yield). The reference yield is the yield in the absence of any water stress and the reduced yield is the yield obtained at the end of the season hit by a drought in a specific crop growth stage.

	Vegetative		Flowering		Yield formation			
	g1	h1	g2	h2	a	b	c	d
Alessandria	0.57	0.15	0.90	0.24	-3.08	0.72	-4353.67	0.55
Asti	0.53	0.21	0.96	0.34	-1.86	1.07	-648.67	0.51
Brescia	0.43	0.24	1.59	0.87	0.08	15.06	-0.12	0.30
Modena	0.97	0.76	0.97	0.42	-4.33	0.55	-27865.03	0.47
Rovigo	0.54	0.15	1.07	0.40	-6.42	0.38	-46283.35	0.54
Pavia	0.74	0.37	1.45	0.75	-6.42	0.38	-35949.55	0.39
Piacenza	0.61	0.30	0.88	0.29	-2.80	0.84	-18333.11	0.44
Pordenone	0.56	0.15	2.28	1.57	0.08	17.84	-0.09	0.38
Cremona	0.50	0.22	2.62	1.76	-7.35	0.30	-4604.23	0.41
Ferrara	1.03	1.02	1.09	0.53	-4.84	0.50	-36677.04	0.43

The value ranges from 0 to 1, where 1 means the crop is not experiencing a water deficit.

3.6. Derivation of the vulnerability curves

Vulnerability curves for each growth stage are derived according to the following procedure. At first the reference yield for each season s, $Y_{ref,s}$, i.e., the yield in the absence of water stress during all the crop growth stages, is computed. Then, the reduced yield for the same season, $Y_{red,s}$, is derived introducing a water stress in a single growth stage (g) by progressively reducing the precipitation amount during the growth stage g. $Y_{red,s,g}$ is the reduced yield evaluated at the end of the growing season hit by a water stress during the growth stage g. The yield loss, Y_l for the season s hit by a water stress during and the growth stage g is therefore:

$$Y_l = 1 - \frac{Y_{red,s,g}}{Y_{ref,s}} \tag{15}$$

To derive vulnerability curves in which a reduction of 0 in the yield corresponds to the absence of water deficit, a new parameter, the water deficit,Def_w is computed as:

$$Def_w = 1 - f_s \tag{16}$$

The curves obtained for the considered crops and the analysed growing stages are derived by fitting the most appropriate functions to the model output data. Fig. 3.

4. Results and discussion

4.1. Model calibration

At first APSIM is calibrated to evaluate the model's ability in reproducing the observed yield in the Po River basin area. Observed yield are retrieved from the Italian National Institute of Statistics (ISTAT) over the period from 2006 to 2020. Data are aggregated at province level. The period from 2006 to 2013 is used to calibrate the model, while the years from 2014 to 2020 are used for the validation. The use of observed yield data for the crop model calibration process is a common practice, as underlined by Seidel et al. (2018), who reports that nearly 90% of crop model users rely on observed yield to calibrate their model. Fig. 4 reports the results of crop model calibration (a) and validation (b). The R^2 over all the considered provinces for both the calibration and the validation stage is equal to 0.75. When single provinces are considered, the R^2 for the calibration stage ranges from 0.64 (Pordenone) to 0.98 (Cremona), the R^2 for the validation stage from 0.66 (Pordenone) to 0.97 (Ferrara). The discrepancies between the observed and the reported yield for the Pordenone province can be attribute to issues in the reporting of the observed production and harvested area by the Italian Institute of Statistics. Both variables were estimated by expert knowledge during the years from 2009 to 2012 and 2018–2019. However, the results of both model calibration and validation show that the APSIM model can reproduce the observed yield in the Po River basin area, and therefore the model can be used to design maize drought vulnerability curves.

4.2. Vulnerability curves for maize

Based on the water deficit and the associated yield losses computed for the three selected growing stages (e.g., vegetative, flowering and yield formation), drought vulnerability curves for maize were developed as described in Section 3.6. The obtained data points have been fitted to the most appropriate functions. In the case of the vegetative and flowering stages the Michaelis-Menten equation (Eq. 17) has been used:

$$y = \frac{gx}{h + x} \tag{17}$$

while in the case of the yield formation stage the asymmetric logistic has been preferred (Eq. 18):

$$y = c + (d - c)(1 - e^{-e^{b(x-a)}}) \tag{18}$$

Fig.5 shows the curves derived from the water deficit and yield losses for three provinces, one for each soil type. Specifically, Rovigo (loam over clay loam soil), Ferrara (clay loam soil) and Pavia (loam soil) have been selected. Curves for the vegetative stage, the flowering and the yield formation phases have been retrieved.

The data points exhibit a good fit with the selected functions as demonstrated by the high R^2 values, which are significant at 0.01 (Table 3).

Results show that maize is more sensitive to water deficit during the flowering stage, as already reported by Steduto et al. (2012) and underlined by Zhu et al. (2021). The curves for the vegetative stages show similar behavior in all three provinces. The sensitivity to water deficit of the vegetative and yield formation phase is similar in Rovigo (Fig. 4a) and Ferrara (Fig. 4b), while in Pavia (Fig. 4c) the vegetative phase is more sensitive to water deficit than the yield formation phase. This can be related to the fact that the grain yield is already formed during the yield formation phase, and even high water deficits do not affect the crop yield excessively. The results here obtained can be compared with the ones reported in Zhu et al. (2021), even if the study considers four growth stages which do not overlap exactly with the ones of this work and evaluates the yield losses with respect to the DHI, which is an average of the Crop Water Stress Indicator (CWSI) over the growth stage. CWSI is computed as the ratio between actual and potential evapotranspiration through the Aquacrop model. The four stages reported in Zhu et al. (2021) are stage 1, corresponding to the period from sowing to the seventh leaf stage, stage 2 going from the seventh leaf stage to the tasselling stage, stage 3 from the tasselling to the milk stage, and stage 4 from the milk stage to the physiological maturity of the crop. The four growth stages considered in the present study are establishment, which goes from sowing to the plant full emergence from the soil, vegetative, which lasts until the first flowers start to appear, flowering, which includes tassel and silking and yield formation, which includes grain filling and ripening. In the case of the Po river basin, the plant never experience a water stress during the first growth stage (establishment or stage 1), while low yield reduction are reported in Zhu et al. (2021). During stage 2 (vegetative) yield losses in Zhu et al. (2021) reach 60% while in this study are around 40%, while in stage 3 (flowering) maximum yield reduction in this study is high (around 85%) with respect to Zhu et al. (2021), in which yield losses amount at about 60%. Yield losses in the final stage are again higher in this study (between 40% and 60%) than in Zhu et al. (2021), where in the final growth stage no losses are reported for every value of the DHI.

The differences between the two studies can be attributed to various reasons. At first, as already described, the four stages do not overlap exactly. Secondly, the climate and the rainfall patterns of China are different from the ones of the Po River basin. Finally, as underlined by Zhu et al. (2021), in the Chinese case study the amount of sunlight and quality of soil are poor for maize growing.

The soil texture influences the response of the crop to the water deficit in the flowering and the yield formation phases. In the flowering stage for low water deficit, the provinces with a loam soil show lower yield reduction than others, while for high water deficit, the yield reduction is lower in provinces with a clay loam soil texture. A different situation happens during the yield formation phase: in this case for all the water deficits, the provinces with a loam over clay loam soil show a higher yield reduction than the others. This behaviour can be explained by the properties of the different soil textures. To this end, Groenendyk et al. (2015) examined whether soil textural classifications could be useful proxies for hydraulic properties over a range of hydrologic conditions and developed an alternative approach to soil classification that can improve both quantitative analyses and visual interpretations of landscape function. Fig. 5a illustrates the USDA soil classification, whereas Fig. 5b shows the hydraulic conductivity for different soil textures retrieved from simulations considering only the uppermost 30 cm of soil (Groenendyk et al., 2015).

The two panels show differences in hydraulic conductivity between loam and clay loam soils. The loam soil type has a greater hydraulic conductivity than the clay loam one. Groenendyk et al. (2015) work shows also that soils with a greater value in hydraulic conductivity have also a greater capacity in infiltration and drainage. Oppositely, soils with a lower value of hydraulic conductivity, have the capability to retain water at a microscopic scale, thus guaranteeing water availability for plants' roots for longer periods of time than other kind of soils. During drought or water stress periods, this feature results in a longer water availability at the root zone, meaning that these kinds of soils have the ability to support plants' resilience to prolonged water stress. In our case, this finding can explain why for, higher values of water deficits, clay loam soils show less yield reduction than the other ones, especially in the flowering growth stage. During the vegetative stage the soil texture does not play a significant influence on the response of maize to water stress, probably because this growth stage shows less sensitivity to water stress, and consequently the influence of soil texture is less evident. As shown in Fig. 6, the maximum yield loss that can be obtained during the vegetative stage ranges from 0.26 (Brescia) to 0.42 (Modena). Flowering remains the most critical stage in all the provinces, with the maximum yield losses ranging from 0.67 (Modena) to 0.94 (Cremona). The yield formation phase shows the highest variability. Maximum yield losses range from 0.35 (Brescia) to 0.54 (Alessandria). Fig. 7 shows a vulnerability matrix that summarizes the main results when the maximum water stress (Water deficit equal to 1) is considered. Yield losses are computed through Eq. 17 for the vegetative and flowering phase and Eq. 18 for the yield formation phase using the constant values reported in Table A.1. Yield losses in the vulnerability matrix are expressed as percentage and the values represents the average yield loss over provinces with the same soil texture. The establishment phase never went under water stress in the Po River basin in the considered simulations, therefore no yield losses are assigned to this phase. During the establishment, maize needs small amount of water that can be easily provided by all the three different considered soil types, which, as already mentioned, have the capability to retain water due to their characteristic values of hydraulic conductivity. Flowering is the most sensitive stage to water deficit, and high yield losses are reported in case of water stress during this period, particularly in case of loam and loam over clay loam soils. The vegetative stage is not highly influenced by the soil texture, while the yield formation phase is less sensitive to water deficit in case of a loam soil texture. The proposed classification could be used to support water management strategies to improve cooperation among stakeholders, which is essential to ensure water and food security in the area (Lu et al., 2021).

5. Conclusions

Stage specific drought vulnerability curves for maise tailored to the Po River basin context have been developed. Establishment, Vegetative, Flowering and Yield formation stages have been considered. The curves have been developed for ten provinces with different soil texture. APSIM was used to compute the reference yield (the yield in the absence of any water stress during all the crop growth stages), the yield losses due to water stress and the water deficit associated with periods of drought happening during each of the crop growth stages. The results of APSIM calibration and validation were satisfactory. The water deficit and the associated yield losses have been used to construct the vulnerability curves for the four growth stages. The establishment phase never went under waters stress in the climatic conditions of the Po Valley, because the amount of the water required by the crop in this phase is small and

can be easily provided by the soil. Overall, flowering has turned out to be the most sensitive stage to water deficit in all the provinces, in agreement with other studies, while the yield formation and the vegetative stage were less sensitive to the water stress. The soil texture plays an influence on the response of the crop to the water deficit, mainly in the flowering and the yield formation phases. During flowering, for high water deficits the yield reduction is lower in the provinces with a clay loam soil texture with respect to the others, while for low water deficits the provinces with a loam soil show lower yield losses. In the yield formation phase the provinces with a loam soil show a lower yield reduction than the provinces with a loam over clay loam soil for all the water deficits. During the vegetative phase the soil texture did not play a significant role in determining the yield reduction associated with high water deficits. The achieved results could foster a sustainable use of water resources in agriculture by suggesting the most appropriate time to rely on irrigation.

Funding statement

This work was supported by the Italian Ministry of Education, within the framework of the project Dipartimenti di Eccellenza 2018–2022 (L.11/12/2016 n.232) at IUSS Pavia and by the Regione Lombardia within the framework of the project IUSS Data Center (DGR n.XI/3776/2020).

Declaration of Competing Interest

The authors declare that they have no known competing financial interests or personal relationships that could have appeared to influence the work reported in this paper.

Appendix A. Vulnerability curves parameters

See: Table A.1.

References

Allen, R.G., Pereira, L.S., Raes, D., Smith, M., 1988. Crop evapotranspiration: guidelines for computing crop water requirements. FAO Irrig. Drain. Pap. 56., Italy.: FAO. ⟨http://www.climasouth.eu/sites/default/files/FAO56.pdf⟩.

Food and Agriculture Organization, 2012. Introducing AquaCrop. ⟨https://www.fao.org/documents/card/en/c/ba35b63c-596a-467d-95fe-dfcfca6da2a9/⟩.

Food and Agriculture Organization, 2017. AquaCrop, the crop water productivity model. ⟨http://www.fao.org/3/a-i7455e.pdf⟩.

Food and Agriculture Organization, 2017: The Impact of disasters and crises on agriculture and food Security. Technical Report; Rome; 2018.⟨https://www.fao.org/documents/card/en/c/I8656EN/⟩.

APSIM, SoilWat. 2018. ⟨https://www.apsim.info/documentation/model-documentation/soil-modules-documentation/soilwat/⟩.

European Environment Agency (EEA), 2018. Corine Land Cover. 2021.⟨https://land.copernicus.eu/pan-european/corine-land-cover⟩.

Italian National Institute of Statistics.I.stat.2021.⟨http://dati.istat.it/⟩.

Bachmair, S., Svensson, C., Hannaford, J., Barker, L.J., Stahl, K., 2016. A quantitative analysis to objectively appraise drought indicators and model drought impacts. Hydrol. Earth Syst. Sci. 20, 2589–2609. https://doi.org/10.5194/hess-20-2589-2016.

Bachmair, S., Svensson, C., Prosdocimi, I., Hannaford, J., Stahl, K., 2017. Developing drought impact functions for drought risk management. Nat. Hazards Earth Syst. Sci. 17 (11), 1947–1960. https://doi.org/10.5194/nhess-17-1947-2017. ⟨https://nhess.copernicus.org/articles/17/1947/2017/⟩.

Baronetti, A., González-Hidalgo, J.C., Vicente-Serrano, S.M., Acquaotta, F., Fratianni, S., 2020. A weekly spatio-temporal distribution of drought events over the Po Plain (North Italy) in the last five decades. Int. J. Clim. 40 (10), 4463–4476. https://doi.org/10.1002/joc.6467.

Beck, H.E., Zimmermann, N.E., McVicar, T.R., Vergopolan, N., Berg, A., Wood, E.F., 2018. Present and future Köppen-Geiger climate classification maps at 1-km resolution. Sci. Data 5 (1), 180214. https://doi.org/10.1038/sdata.2018.214. ⟨http://www.nature.com/articles/sdata2018214⟩.

Bennett, D.R., Harms, T.E., 2011. Crop yield and water requirement relationships for major irrigated crops in Southern Alberta. Can. Water Resour. J. 36 (2), 159–170. https://doi.org/10.4296/cwrj3602853.

Blöschl, G., Sivapalan, M., Wagener, T., Viglione, A., Savenije, H., 2013. Runoff Prediction in Ungauged Basins: Synthesis across Processes. Places and Scales. Cambridge University Press, Cambridge. https://doi.org/10.1017/CBO9781139235761.

Borzì, I., Bonaccorso, B., 2021. Quantifying groundwater resources for municipal water use in a data-scarce region. Hydrology 8 (4), 184. https://doi.org/10.3390/hydrology8040184. ⟨https://www.mdpi.com/2306-5338/8/4/184⟩.

Borzì, I., Bonaccorso, B., Fiori, A., 2019. A modified IHACRES rainfall-runoff model for predicting the hydrologic response of a river basin connected with a deep groundwater aquifer. Water 11 (10). https://doi.org/10.3390/w11102031.

Borzì, I., Bonaccorso, B., Aronica, G.T., 2020. The role of dem resolution and evapotranspiration assessment in modeling groundwater resources estimation: a case study in sicily. Water 12 (11), 1–15. https://doi.org/10.3390/w12112980.

von Christierson, B., Hannaford, J., Lonsdale, K., Parry, S., Rance, J., Wade, S., Jones, P., 2012. Impacts of Long Droughts On Water Resources. Environment Agency, Bristol.

Cesarini, L., Figueiredo, R., Monteleone, B., Martina, M.L.V., 2021C. The potential of big data and machine learning for weather index insurance. Nat. Hazards Earth Syst. Sci. 21, 2379–2405. https://doi.org/10.5194/nhess-21-2379-2021.

Cornes, R.C., van der Schrier, G., van den Besselaar, E.J., Jones, P.D., 2018. An ensemble version of the E-OBS temperature and precipitation data sets. J. Geophys Res-Atmos. 123 (17), 9391–9409. https://doi.org/10.1029/2017JD028200.

Costantini, E., Barbetti, R., Fantappiè, M., L'Abate, G., Lorenzetti, R., 2013. Magini. Pedodiversity. In: Costantini, E.A., Dazzi, C. (Eds.), The Soils of Italy. Dordrecht: Springer. World Soils Book Series, Netherlands, pp. 105–178. https://doi.org/10.1007/978-94-007-5642-7.

Crespi, A., Borghi, A., Facchi, A., Gandolfi, C., Maugeri, M., 2020. Spatio-temporal variability and trends of drought indices over lombardy plain (Northern Italy) from meteorological station records (1951-2017). Ital. J. Agrometeorol. 2020 (2), 3–18. https://doi.org/10.13128/ijam-1101.

Croke, B.F., Smith, A.B., Jakeman, A.J., 2002. A one-parameter groundwater discharge model linked to the IHACRES rainfall-runoff model. Int. Congr. Environ. Model. Softw. 256. ⟨https://scholarsarchive.byu.edu/iemssconference/2002/all/256⟩.

Davis R., Bennett H.H., 1927. Grouping of soils on the basis of mechanical analysis.1927. https://www.iuss.org/meetings-events/world-soil-congress/.

Groenendyk, D.G., Ferré, T.P., Thorp, K.R., Rice, A.K., 2015. Hydrologic-process-based soil texture classifications for improved visualization of landscape function. Plos One 10 (6). https://doi.org/10.1371/journal.pone.0131299.

Guo, H., Zhang, X., Lian, F., Gao, Y., Lin, D., Wang, J., 2016. Drought risk assessment based on vulnerability surfaces: A case study of maize. Sustain. -Basel 8 (8). https://doi.org/10.3390/su8080813.

Hengl, T., Mendes de Jesus, J., Heuvelink, G.B.M., Ruiperez Gonzalez, M., Kilibarda, M., Blagotić, A., Shangguan, W., Wright, M.N., Geng, X., Bauer-Marschallinger, B., Guevara, M.A., Vargas, R., MacMillan, R.A., Batjes, N.H., Leenaars, J.G.B., Ribeiro, E., Wheeler, I., Mantel, S., Kempen, B., 2017. SoilGrids250m: Global gridded soil information based on machine learning. Plos One 12 (2), e0169748. https://doi.org/10.1371/journal.pone.0169748. ⟨https://dx.plos.org/10.1371/journal.pone.0169748⟩.

Ivković K.M.J. Modelling Groundwater-River Interactions for Assessing Water Allocation Options. Technical Report; 2006.⟨https://openresearch-repository.anu.edu.au/bitstream/1885/49342/2/02whole.pdf⟩.

Jakeman, A.J., Hornberger, G.M., 1993. How much complexity is warranted in a rainfall-runoff model? Water Resour. Res 29 (8), 2637–2649. https://doi.org/10.1029/93WR00877.

Jayanthi, H., Husak, G.J., Funk, C., Magadzire, T., Adoum, A., Verdin, J.P., 2014. A probabilistic approach to assess agricultural drought risk to maize in Southern Africa and millet in Western Sahel using satellite estimated rainfall. Int. J. Disast Risk Re 10 (PB), 490–502. https://doi.org/10.1016/j.ijdrr.2014.04.002.

Jia, H., Wang, J., Cao, C., Pan, D., Shi, P., 2012. Maize drought disaster risk assessment of China based on EPIC model. Int J. Digit Earth 5 (6), 488–515. https://doi.org/10.1080/17538947.2011.590535. ⟨http://www.tandfonline.com/doi/abs/10.1080/17538947.2011.590535⟩.

Kamali, B., Abbaspour, K.C., Lehmann, A., Wehrli, B., Yang, H., 2018. Spatial assessment of maize physical drought vulnerability in sub-Saharan Africa: linking drought exposure with crop failure. Environ. Res. Lett. 13 (7), 074010 https://doi.org/10.1088/1748-9326/aacb37. ⟨https://iopscience.iop.org/article/10.1088/1748-9326/aacb37⟩.

Kamara, A.Y., Menkir, A., Badu-Apraku, B., Ibikunle, O., 2003. The influence of drought stress on growth, yield and yield components of selected maize genotypes. J. Agr. Sci. 141 (1), 43–50. https://doi.org/10.1017/S0021859603003423.

Keating, B., Carberry, P., Hammer, G., Probert, M., Robertson, M., Holzworth, D., Huth, N., Hargreaves, J., Meinke, H., Hochman, Z., McLean, G., Verburg, K., Snow, V., Dimes, J., Silburn, M., Wang, E., Brown, S., Bristow, K., Asseng, S., Chapman, S., McCown, R., Freebairn, D., Smith, C., 2003. An overview of APSIM, a model designed for farming systems simulation. Eu J. Agron. 18 (3–4), 267–288. https://doi.org/10.1016/S1161-0301(02)00108-9. ⟨https://linkinghub.elsevier.com/retrieve/pii/S1161030102001089⟩.

Korres, N.E., Norsworthy, J.K., Burgos, N.R., Oosterhuis, D.M., 2017. Temperature and drought impacts on rice production: An agronomic perspective regarding short- and long-term adaptation measures. Water Resour. Rur Dev. 9, 12–27. https://doi.org/10.1016/j.wrr.2016.10.001.

Lu, Y., Tian, F., Guo, L., Borzì, I., Patil, R., Wei, J., Liu, D., Wei, Y., Yu, D.J., Sivapalan, M., 2021. Socio-hydrologic modeling of the dynamics of cooperation in the transboundary Lancang-Mekong River. Hydrol. Earth Syst. Sci. 25 (4), 1883–1903. https://doi.org/10.5194/hess-25-1883-2021.

Monteith, J., Greenwood, D., 1986. How do crops manipulate water supply and demand? Philos. Trans. R. Soc. A 316 (1537), 245–259. https://doi.org/10.1098/rsta.1986.0007. ⟨https://royalsocietypublishing.org/doi/10.1098/rsbm.1986.0012https://royalsocietypublishing.org/doi/10.1098/rsta.1986.0007⟩.

Monteleone, B., Bonaccorso, B., Martina, M., 2020. A joint probabilistic index for objective drought identification: the case study of Haiti. Nat. Hazards Earth Syst. Sci. 20, 471–487. https://doi.org/10.5194/nhess-20-471-2020.

Musolino, D., de Carli, A., Massarutto, A., 2017. Evaluation of socio-economic impact of drought events: the case of Po river basin. Eur. Countrys. 9 (1), 163–176. https://doi.org/10.1515/euco-2017-0010. ⟨https://content.sciendo.com/view/journals/euco/9/1/article-p163.xml⟩.

Musolino, D., Vezzani, C., Massarutto, A., 2018. Drought Management in the Po River Basin, Italy. In: Iglesias, A., Assimacopoulos, D., Van Lanen, H. (Eds.), Drought: Science and Policy, 1st ed.,. John Wiley and Sons Ltd, pp. 201–215. https://doi.org/10.1002/9781119017073.ch11.

Naumann, G., Spinoni, J., Vogt, J.V., Barbosa, P., 2015. Assessment of drought damages and their uncertainties in Europe. Environ. Res Lett. 10, 12.

Palatella, L., Miglietta, M.M., Paradisi, P., Lionello, P., 2010. Climate Change assessment for Mediterranean agricultural areas by statistical downscaling. Nat. Hazards Earth Syst. Sci. 10 (7), 1647–1661. https://doi.org/10.5194/nhess-10-1647-2010.

Papathoma-Köhle, M., 2016. Vulnerability curves vs. Vulnerability indicators: Application of an indicator-based methodology for debris-flow hazards. Nat. Hazards Earth Syst. Sci. 16 (8), 1771–1790. https://doi.org/10.5194/nhess-16-1771-2016.

Regione Lombardia.Norme tecniche agronomiche per i Regolamenti 1182/07/CE, 1234/07/CE, 543/11/UE, 1308/13/UE: Parte speciale.2020a.

Regione Lombardia.Sistemi di produzione integrata nelle filiere agroalimentari: Norme tecniche agronomiche per i Regolamenti 1182/07/CE, 1234/07/CE, 543/11/UE, 1308/13/UE.2020b.

Reyenga, P., Howden, S., Meinke, H., McKeon, G., 1999. Modelling global change impacts on wheat cropping in south-east Queensland, Australia. Environ. Model Softw. 14 (4), 297–306. https://doi.org/10.1016/S1364-8152(98)00081-4. ⟨https://linkinghub.elsevier.com/retrieve/pii/S1364815298000814⟩.

Saxton, K.E., Rawls, W.J., Romberger, J.S., Papendick, R.I., 1986. Estimating Generalized Soil-water Characteristics from Texture. Soil Sci. Soc. Am. J. 50 (4), 1031–1036. https://doi.org/10.2136/sssaj1986.03615995005000040039x. ⟨https://acsess.onlinelibrary.wiley.com/doi/abs/10.2136/sssaj1986.03615995005000040039x⟩.

Schaperow, J.R., Li, D., Margulis, S.A., Lettenmaier, D.P., 2021. A near-global, high resolution land surface parameter dataset for the variable infiltration capacity model. Sci. Data 8 (1). https://doi.org/10.1038/s41597-021-00999-4.

Seidel, S.J., Palosuo, T., Thorburn, P., Wallach, D., 2018. Towards improved calibration of crop models - Where are we now and where should we go? Eu J. Agron. 94 (February), 25–35. https://doi.org/10.1016/j.eja.2018.01.006.

Shaban, A., Khawlie, M., Abdallah, C., 2006. Use of remote sensing and GIS to determine recharge potential zones: The case of Occidental Lebanon. Hydrogeol. J. 14 (4), 433–443. https://doi.org/10.1007/s10040-005-0437-6.

Shaxson F., Barber R. Optimizing soil moisture for plant production. The significance of soil porosity. FAO Soils Bulletin 79. Technical Report; 2003.

, 2017Soil Science Division Staff.Soil Survey Manual, USDA. Usda handb ed. Washington, D.C.: Government Printing Office, 2017.https://www.nrcs.usda.gov/wps/portal/nrcs/detailfull/soils/ref/?cid=nrcs142p2_054262.

Steduto P., Hsiao T.C., Fereres E., Raes D. Crop yield response to water. Rome, 2012.

Storck, P., Bowling, L., Wetherbee, P., Lettenmaier, D., 1998. Application of a GIS-based distributed hydrology model for prediction of forest harvest effects on peak stream flow in the Pacific Northwest. Hydrol. Proces. 12 (6), 889–904. https://doi.org/10.1002/(SICI)1099-1085(199805)12:6<889::AID-HYP661>3.0.CO;2-P. ⟨https://onlinelibrary.wiley.com/doi/10.1002/(SICI)1099-1085(199805)12:63C889::AID-HYP6613E3.0.CO;2-P⟩.

Su, P., Li, S., Wang, J., Liu, F., 2021. Vulnerability assessment of maize yield affected by precipitation fluctuations: a northeastern united states case study. Land 10 (11). https://doi.org/10.3390/land10111190.

Tanner, C.B., Sinclair, T.R., 2015. Efficient water use in crop production: research or research? In: Taylor, H., Jordan, W., Sinclair, T. (Eds.), Limitations to Efficient Water Use In Crop Production. American Society of Agronomy, Madison, pp. 1–27. https://doi.org/10.2134/1983.limitationstoefficientwateruse.c1.

Viglione, A., Parajka, J., Rogger, M., Salinas, J.L., Laaha, G., Sivapalan, M., Blöschl, G., 2013. Comparative assessment of predictions in ungauged basins - Part 3: runoff signatures in Austria. Hydrol. Earth Syst. Sci. 17 (6), 2263–2279. https://doi.org/10.5194/hess-17-2263-2013. ⟨https://hess.copernicus.org/articles/17/2263/2013/⟩.

Wang, Y., Zhao, W., Zhang, Q., 2019. bi Yao Y. Characteristics of drought vulnerability for maize in the eastern part of Northwest China. Sci. Rep. 9 (1), 1–9. https://doi.org/10.1038/s41598-018-37362-4.

Webb, R.S., Rosenzweig, C.E., Levine, E.R., 1993. Specifying land surface characteristics in general circulation models: Soil profile data set and derived water-holding capacities. Glob. Biogeochem. Cy 7 (1), 97–108. https://doi.org/10.1029/92GB01822. ⟨http://doi.wiley.com/10.1029/92GB01822⟩.

Werner, A.D., Gallagher, M.R., Weeks, S.W., 2006. Regional-scale, fully coupled modelling of stream-aquifer interaction in a tropical catchment. J. Hydrol. 328 (3), 497–510. https://doi.org/10.1016/j.jhydrol.2005.12.034.

Wilhelmi, O.V., Wilhite, D.A., 2002. Assessing vulnerability to agricultural drought: a Nebraska case study. Nat. Hazards 25 (1), 37–58. https://doi.org/10.1023/A:1013388814894.

Wilson, M., Henderson-Sellers, A., 1985. A global archive of land cover and soils data for use in general circulation climate models. J. Clim. 5 (2), 119–143. https://doi.org/10.1002/joc.3370050202. ⟨https://rmets.onlinelibrary.wiley.com/doi/abs/10.1002/joc.3370050202⟩.

Wu, Y., Guo, H., Zhang, A., Wang, J., 2021. Establishment and characteristics analysis of a crop-drought vulnerability curve: a case study of European winter wheat. Nat. Hazards Earth Syst. Sci. 21 (4), 1209–1228. https://doi.org/10.5194/nhess-21-1209-2021.

Yang, J., Wu, J., Liu, L., Zhou, H., Gong, A., Han, X., Zhao, W., 2020. Responses of winter wheat yield to drought in the north china plain: spatial-temporal patterns and climatic drivers. Water 12 (11), 3094. https://doi.org/10.3390/w12113094. ⟨https://www.mdpi.com/2073-4441/12/11/3094⟩.

Yin, Y., Zhang, X., Lin, D., Yu, H., Wang, J., Shi, P., 2014. GEPIC-V-R model: a GIS-based tool for regional crop drought risk assessment. Agr. Water Manag. 144, 107–119. https://doi.org/10.1016/j.agwat.2014.05.017.

Yin, Y., Zhang, X., Yu, H., Lin, D., Wu, Y., Wang, J., 2015. Mapping Drought Risk (Maize) of the World. In: Shi, P., Kasperson, R. (Eds.), World Atlas of Natural Disaster Risk. Springer-Verlag Berlin Heidelberg and Beijing Normal University Press; number July 2017, pp. 211–226. https://doi.org/10.1007/978-3-662-45430-5_11.

Zhang, X., Guo, H., Yin, W., Wang, R., Li, J., Yue, Y., Wang, J., 2015a. Mapping Drought Risk (Wheat) of the World. In: Shi, P., Kasperson, R. (Eds.), World Atlas of Natural Disaster Risk. Springer-Verlag Berlin Heidelberg and Beijing Normal University Press, pp. 227–242. https://doi.org/10.1007/978-3-662-45430-5_12.

Zhang, X., Lin, D., Guo, H., Wu, Y., Wang, J., 2015b. Mapping Drought Risk (Rice) of the World. In: Shi, P., Kasperson, R. (Eds.), World Atlas of Natural Disaster Risk. Springer-Verlag Berlin Heidelberg and Beijing Normal University Press; number July 2017, pp. 243–258. https://doi.org/10.1007/978-3-662-45430-5_13.

Zheng B., Chenu K., Doherty A., Chapman S. The APSIM-Wheat Module (7.5 R3008). Technical Report; 2015.⟨https://www.apsim.info/wp-content/uploads/2019/09/WheatDocumentation.pdf⟩.

Zhu, X., Xu, K., Liu, Y., Guo, R., Chen, L., 2021. Assessing the vulnerability and risk of maize to drought in China based on the AquaCrop model. Agr. Syst. 189 (September 2020), 103040 https://doi.org/10.1016/j.agsy.2020.103040.